

MIT Open Access Articles

*Climate-Conscious Urban Growth Mitigates
Urban Warming: Evidence from Shenzhen, China*

The MIT Faculty has made this article openly available. **Please share**
how this access benefits you. Your story matters.

Citation: Zhou, Yulun, Huang, Bo, Wang, Jionghua, Chen, Bin, Kong, Hui et al. 2019. "Climate-Conscious Urban Growth Mitigates Urban Warming: Evidence from Shenzhen, China." *Environmental Science and Technology*, 53 (20).

As Published: <http://dx.doi.org/10.1021/acs.est.9b01645>

Publisher: American Chemical Society (ACS)

Persistent URL: <https://hdl.handle.net/1721.1/133019>

Version: Author's final manuscript: final author's manuscript post peer review, without publisher's formatting or copy editing

Terms of use: Creative Commons Attribution-Noncommercial-Share Alike



Climate-Conscious Urban Growth Mitigates Urban Warming: Evidence from Shenzhen, China

A Preprint - Environmental Science & Technology
[Subject to Changes in the final version]
Please Cite: <http://dx.doi.org/10.1021/acs.est.9b01645>

Yulun Zhou^{1†}, Bo Huang^{12†*}, Jionghua Wang²³, Bin Chen⁴, Hui Kong⁵, Leslie Norford⁶

¹ Department of Geography & Resource Management, The Chinese University of Hong Kong, Hong Kong, China

² Institute of Space and Earth Information Science, The Chinese University of Hong Kong, Hong Kong, China

³ Faculty of Geosciences and Environmental Engineering, Southwest Jiaotong University, Chendu 611756, China

⁴ Department of Land, Air and Water Resources, University of California, Davis, CA 95616, USA

⁵ Singapore–MIT Alliance for Research and Technology (SMART), Singapore 138602

⁶ Department of Architecture, Massachusetts Institute of Technology, Cambridge, MA 02139, USA

† Yulun Zhou and Bo Huang contributed equally to this manuscript and should be considered co-first authors.

* Corresponding author: Bo Huang: bohuang@cuhk.edu.hk

Abstract

Urban growth comes with significant warming impacts and related increases in air pollution concentrations, so many cities have implemented growth management to minimize ‘sprawl’ and its environmental consequences. However, controlling the amount of growth is costly. Therefore, in this paper, we focus on urban warming and investigate whether climate-conscious urban growth planning (CUGP), i.e., urban growth with the same magnitude but optimized spatial arrangements, brings significant mitigation effects. First, the classical spatial multi-objective land-use optimization (SMOLA) model is improved by integrating the spatially-, diurnally-, and compositionally-varying associations between land-use and their warming impacts. Then, we solve the improved model using the non-dominated genetic algorithm (NSGA-II) to generate urban growth plans with minimal warming impacts and minimal cost of change without reducing the amount of urban growth. Results show that climate-conscious urban growth brings $33.3 \pm 4.6\%$ less warming impacts compared to unplanned urban growth in Shenzhen, China, and suggest a compact and spatially equalized development pattern. This study provides evidence that spatial planning tools such as the CUGP can help mitigate human impacts on the environment. Meanwhile, the improved SMOLA model could be applied to balance urban development and other environmental consequences such as air pollution.

Acknowledgement

Appreciation goes to Qianhui Liang (MIT) and Michael Seidenkühnel for engaging in artistic designs of the cover art. This study was supported by National Key R&D Program of China (2017YFB0503605), which is gratefully acknowledged.

42 **1. INTRODUCTION**

43 One of the most direct environmental consequences arising from massive global urbanization is
44 urban warming, which leads to increased cooling energy demand, increased air pollution, and
45 elevated public health risks associated with human exposure to high ambient temperatures. Urban
46 heat island (UHI), the long-recognized effect that cities have higher air temperatures than their
47 surrounding countrysides, is an extreme case of how land-use changes modify regional climate¹.
48 Reported in many global cities, exacerbated UHIs can be as dramatic as 10°C depending on the
49 local weather conditions^{2,3}. Such intense heat stress brings substantial health risks to urban dwellers,
50 particularly during excessive heat events (EHEs), i.e., heat waves⁴. Exposure to extreme heat leaves
51 the elderly, in particular, at risk of suffering heat cramps, heat exhaustion, and heatstroke.
52 Temperature is also found to exert the strongest and most stable influence on PM_{2.5} concentrations
53 in all seasons amongst meteorological factors⁵. Researchers have long sought to mitigate urban
54 warming, and many studies have suggested such promising mitigation measures as green roof,
55 reflective streets, and increased green space with optimized positioning⁶⁻¹². However, existing
56 studies on mitigating urban warming paid insufficient attention to making low-cost improvements
57 to future urban growth plans. Also, many studies have not considered the extreme case of EHEs
58 when heat-related deaths are most likely to occur¹³.

59
60 Urban growth – the expansion of a metropolitan or suburban area into the surrounding environment
61 – is an economic phenomenon inextricably linked with the process of urbanization¹⁴. Urban lands
62 – developed, built-up areas with a density of human structures such as houses, buildings, and roads
63 – are primary heat sources in cities¹⁵. Urban growth increases urban temperatures significantly by
64 reducing green space, altering surface albedo and geometry compared to rural surfaces¹⁵. The
65 associations between urban land-uses and their warming effects have been studied extensively¹⁶⁻¹⁸.
66 Urban growth is found to be consistently associated with a substantial temperature increase^{11,19,20},
67 and in newly urbanized areas of the city, such an increase can be comparable to the increase under
68 the highest greenhouse gas emissions scenario (RCP8.5)²¹. Such temperature increases vary with
69 time of day¹⁶ and land-use compositions^{17,22}, i.e., the abundance and variety of land cover features.
70 The development density of urban lands is a critical compositional factor in the variability of urban
71 temperatures; higher temperatures often occur in dense urban areas, where the population density is
72 also higher. However, nearly half of the studies on urban warming impacts of urbanization have
73 ignored the variability in urban development density²³, which may underestimate the magnitude of
74 the warming impacts of urban lands, especially in the densest areas. Besides the composition, the
75 spatial configuration^{17,24,25} of urban lands, that is, their spatial arrangement and distribution, can
76 affect the magnitude of urban warming. For example, comparison results from regional climate
77 simulations indicate that a compact mode of urban growth has significant potential in moderating
78 the mean-areal urban warming^{26,27}. Empirical data analyses also show that sprawling cities are more
79 vulnerable to heat stress during EHEs compared to their compact counterparts⁴.

80 Future urban growth with careful spatial arrangements may mitigate its warming impacts without
81 having to reduce the total amount of the growth, yet we know little about the optimal effectiveness
82 and efficiency of this approach. Recent developments in spatial optimization methods have made it
83 possible to formulate the land-use planning problem as a spatial multi-objective land-use allocation
84 (SMOLA) problem guided by a selected set of objectives about sustainability.

85
86 Land-use optimization problems were first articulated in the 1960s when the linear programming
87 (LP) model of land-use design was proposed²⁸. Later developments in spatial optimization methods
88 have introduced the location-allocation model²⁹ and their generalization to multi-objective
89 optimizations in which the trade-offs among multiple objectives were considered^{30–34}. In early
90 practices of solving multi-objective problems using LP models³⁵, it was a major issue to quantify
91 the relative weights of the selected objectives. Then, SMOLA models based on Pareto optimality
92 were proposed and became popular for land-use problems^{11,34,36–39}, since the objectives were
93 independent of each other, no weights were needed, and a series of equally good solutions, called
94 “the Pareto Front”, can be generated simultaneously. Since the environmental impacts of
95 urbanization are increasingly drawing public attention, there has been growing interest in the use of
96 SMOLA models to mitigate negative impacts. For instance, Zhang and Huang¹¹ first applied a
97 spatial multi-objective optimization model to mitigate urban heat island effects. Zhang et al.¹²
98 demonstrated that increased greenness with optimized distributions could be a useful urban warming
99 mitigation measure. However, most existing studies ignored the heterogeneity in the objective
100 functions, i.e., the empirical models used to assess the environmental impacts of optimized plans,
101 except for Zhang et al.¹², who included different assessment functions for daytime and nighttime
102 temperatures and enabled identification of trade-off solutions that balance diurnal cooling benefits.
103 Therefore, the assumption that these objective functions are fixed is not always valid, especially
104 when dealing with environmental objectives, since such environmental responses as urban warming
105 could contain substantial spatial, diurnal and compositional variances. Not considering such
106 heterogeneous associations in environment-related spatial optimization problems may lead to two
107 main problems: 1) the fixed functions may not provide accurate environmental impact assessments
108 of the optimized plans, and so the SMOLA model may fail to generate plans with real improvements.
109 2) the solution space is limited by the fixed functions, leading to limited improvements in
110 environmental objectives.

111
112 Therefore, this paper has two objectives. First, we investigate the spatially-, diurnally-, and
113 compositionally-varying temperature-land-use relationships and improve the classical SMOLA
114 model by integrating such varying relationships. Second, using the improved SMOLA model, we
115 systematically examine the effectiveness and cost of the so-called climate-conscious urban growth
116 planning (CUGP) as a possible mitigation measure for urban warming. This investigation is
117 significant and timely for two main reasons:

118

119 1) If planned wisely, the expected urban growth in the next two decades will provide a
120 significant opportunity for urban warming mitigation.

121 2) It is now possible to tap the potential climate benefits from spatial urban growth planning
122 with extensive results on temperature-land-use relationships and recent developments in
123 spatial optimization.

124 The remainder of this paper is organized as follows. Section 2 introduces the materials and methods
125 used in the investigation. Sections 3 and 4 present results and discussions on climate-conscious
126 urban growth based on our case study in Shenzhen, China. Section 5 present the conclusions.

127

128 2. MATERIAL AND METHODS

129 The study was conducted in two steps. First, we modeled the temperature-land-use relationship to
130 allow the warming effects of urban growth to be estimated empirically. Then, we measured the
131 effectiveness of the CUGP for urban warming mitigation by estimating the warming impacts of
132 urban growth with (Experimental Scenario) and without (Baseline Scenario) optimized spatial
133 arrangements and comparing them with each other (Figure S1).

134

135 Notations

136 i $i \in \{1, 2, \dots, N\}$; cell locations, where N is the total number of cells in the study area.

137 L_i land-use at location i in the *status quo*.

138 L'_i land-use at location i in the optimized plan.

139 I_i land-use intensity index at location i in the *status quo*.

140 I'_i land-use intensity index at location i in the optimized plan.

141 e_i elevation at location i .

142 s_i slope at location i .

143 P_{lm} the probability that land-use l is an immediate neighbor of land-use m in the *status quo*.

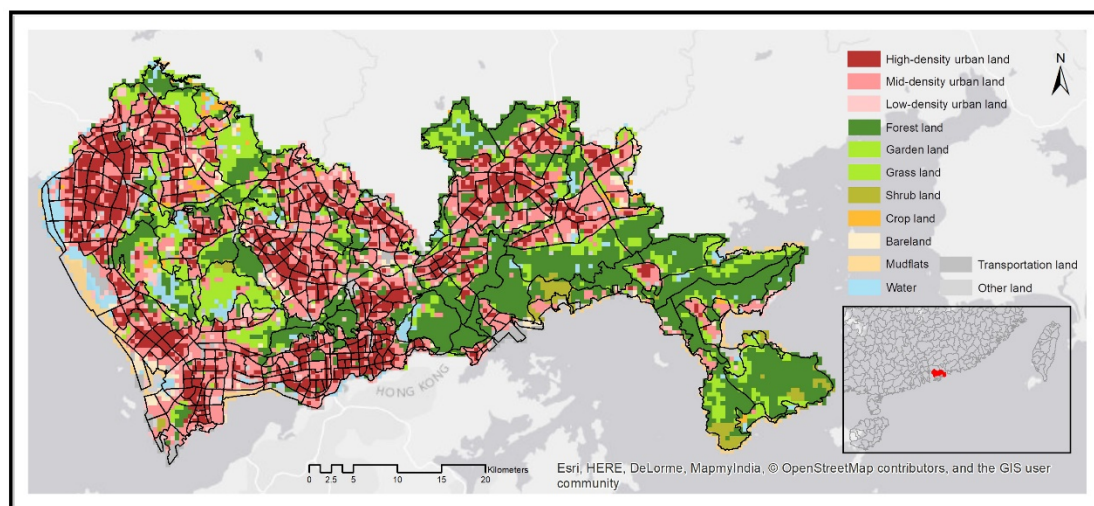
144 P'_{lm} the probability that land-use l is an immediate neighbor of land-use m in the optimized plan.

145 U set of urban lands, including high-, mid-, and low-density urban lands.

146

147 **2.1 Site description.** Shenzhen (east longitude: 113°46' to 114°37', north latitude: 22°27' to 22°52')
148 is a fast-developing post-reform city in south China (Figure 1). As a sub-tropical city with a warm,
149 monsoon-influenced, humid climate, Shenzhen has an average annual temperature of 23°C, and the
150 local summer lasts as long as six months. Luo and Lau³⁸ observed a significant increase in
151 frequency, duration, and intensity of heatwaves in Southern China in the past 40 years; over 50%
152 of the increase was contributed by urbanization. Within territory of 2050 km², the population in
153 Shenzhen has exploded from 2.39 million in 1995 to 10.22 million in 2010 and is projected to reach
154 12.67 million by 2030.

155



156

157 *Figure 1 Land-use map of Shenzhen, a sub-tropical city in south China, in 2010. The used urban subset represents*
158 *sub-districts in Shenzhen⁴⁴.*

159 **2.2 Data.** We focused on the strongest EHE identified in the year of 2010, which lasted 15 days
160 from June 30th to July 15th. The EHE was identified by Luo and Lau³⁸ using observations from 86
161 national ground monitoring stations in Guangdong Province over a 40-year period from 1970 to
162 2010. Satellite-retrieved LST maps and land-use maps were mainly used for the empirical modeling
163 of temperature-land-use relationships. The Land Surface Temperature (LST) was obtained from
164 EOS-Aqua-MODIS C6 composite products (MYD11A2) with a spatial resolution of 30 arc-second
165 (~1 km). The LST map was retrieved from clear-sky (99% confidence) observations at 1:30
166 (nighttime) and 13:30 (daytime) local solar time by using a refined generalized split-window
167 algorithm⁴¹. We resampled the spatial resolution of LST maps to 500m to overlay with the land-
168 use map. Besides, the urban land-use map was retrieved from the official land-use map of Shenzhen
169 in 2010, which is a product of field survey and systematic quality control. We reclassified the urban
170 land category into three subcategories based on their varying development density (please refer to
171 Section S1.2 for more details). The spatial resolution of the land-use map is 500m. A digital
172 elevation map (DEM) of Shenzhen in 2010 with the spatial resolution of 30m was utilized to
173 quantify terrain limits for urban developments. The land-use map and the DEM data are all products
174 of field surveys with systematic quality assurance and control.

175

176 **2.3 The temperature-land-use relationship.** Since the assumption of the existence of a spatially
177 fixed relationship is not always true, especially when dealing with geographical data and such
178 phenomena as urban warming, we applied both global and local modeling methods to estimate the
179 temperature-land-use relationship to find the better-performing model. Urban temperatures can be
180 characterized using air temperature or LST^{15,19}. We used LST as the indicator of urban warming
181 because it is more directly linked to the land-use changes induced by urban growth via the alteration
182 of the physical and biophysical processes¹⁹.

183

184 We took LST as the response variable and calculated 13 land-use indices (Table S1) as predictor
185 variables using the Inversed-Distance-Weighted (IDW) sum to consider not only the local land-use
186 but also its immediate neighbors. We first applied stepwise ordinary least squared regression (OLS)
187 (Eq. 1), one of the most commonly used global modeling approaches, to estimate the temperature-
188 land-use relationship, assuming the existence of a spatially fixed relationship:

189

$$190 \quad LST_i = \sum_l \gamma_l I_{l,i} \quad (\text{Eq. 1})$$

191

192 where i indicates spatial locations within the study area and $I_{l,i}$ is the land-use intensity for the l^{th} land-
193 use type and γ_l is its spatially fixed coefficient. $I_{l,i}$ is the land-use intensity for the l^{th} land-use type
194 and γ_l is its spatially fixed coefficient. The estimated temperature-land-use relationship was self-
195 validated using 10-fold cross-validation (CV). A Python tool was programed for the stepwise OLS
196 estimations equipped with 10-fold CV.

197

198 Then, we applied semi-parametric geographically weighted regression (sGWR)⁴² as the local
199 modeling approach to estimate the temperature-land-use relationship. GWR expands the traditional
200 cross-sectional regression model (Eq. 1) to allow for local variations in the estimated parameters
201 and is found to be a more appropriate analytical framework in conducting research involving
202 multiple spatial data with autocorrelated structures¹⁶. Unlike regular GWR, sGWR allows the
203 simultaneous fitting of mixed spatially varying and fixed coefficients in the same model (Eq. 2), as
204 follows,

205

$$206 \quad LST_i = \sum_k \beta_k(u_i, v_i) I_{k,i} + \sum_l \gamma_l I_{l,i} \quad (\text{Eq. 2})$$

207

208 where $I_{k,i}$ and β_k are the k^{th} local explanatory variable and its coefficient. The coefficients vary
209 depending on the geographical location, (u_i, v_i) . The GWR estimations were implemented using
210 the GWR4 package (version 4.0.90, <http://gwr.maynoothuniversity.ie/gwr4-software/>).

211

212 **2.4 The SMOLA model improved for environmental objectives.** The SMOLA model was
213 improved for considering urban warming or other related environmental objectives by capturing
214 and integrating the spatially-, diurnally-, and compositionally varying environmental responses to
215 land-use changes. In doing so, urban growth plans were optimized based on more reliable
216 environmental impact assessments; the solution space was also enlarged with more combinatorial
217 possibilities. The integration of varying environmental responses into the improved SMOLA model
218 may lead to very different optimization results and larger objective improvements compared to the
219 classical SMOLA model. We solved the SMOLA model using the non-dominated sorting genetic
220 algorithm (NSGA-II), introduced for this purpose by Cao et al.³⁴. Unlike classical multi-objective
221 optimization methods, the NSGA-II algorithm generates a diverse population of equally optimal

222 solutions instead of a single optimal solution, leaving human decision-makers to make the final
223 decision. For details of the NSGA-II-based SMOLA model, please refer to the Supplementary
224 Material.

225

226 **2.5 Warming impacts of unplanned urban growth.** In the baseline scenario, we first simulated
227 urban land-use plans with 10% more unplanned urban land area. The new urban lands were
228 iteratively added to the *status quo* of Shenzhen, 2010 (Figure 1), using a random boundary-based
229 urban growth operator, where all new urban lands were restricted to the boundary area of existing
230 urban lands. The unplanned urban growth was also subject to the three feasibility constraints in
231 Section 2.6. Then, the new urban lands were randomly assigned as high-density, mid-density or
232 low-density urban lands, while the average development density of the entire land-use plan was
233 constrained to be at least equal to or higher than that of the *status quo*. The process was repeated to
234 generate N different plans with unplanned urban growth, where N is the fine-tuned population size
235 in each generation of the spatial optimization model explained in Section 2.4.

236

237 The warming impacts of unplanned urban growth were evaluated empirically using the temperature-
238 land-use relationship estimated in the previous section.

239

240 **2.6 Warming impacts of climate-conscious urban growth.** In the experimental scenario, using an
241 improved SMOLA model, the spatial arrangements of the unplanned urban growth simulated in the
242 previous section were optimized under four objectives: to minimize daytime LST (LST_d), to
243 minimize nighttime LST (LST_n), to maximize land-use compatibility, and to minimize changing
244 cost. Both daytime and nighttime LST were minimized simultaneously to consider the diurnal
245 temperature trade-off¹². Besides the climate objectives, the number of land-use changes was also
246 minimized to maximize the efficiency of optimized changes. In addition, the compatibility between
247 adjacent land-uses was maximized, since there are land-use types that should not exist next to each
248 other (e.g., industrial and residential). Rather than arbitrarily assigning the compatibility weights for
249 each land-use pair (P_{lm}), the weights were learned by summarizing their corresponding appearance
250 probability in the *status quo*.

251

252 Three feasibility constraints proposed to limit the solution space of land-use plans:

- 253 1. *The land demand of Shenzhen shall be satisfied.* The increase of urban land area compared
254 to the *status quo* should be equal to or larger than the required urban growth rate (r_g) of 10%.
255 The average development density cannot be lower than that of the *status quo*.
- 256 2. *Urban development cannot occur on rough terrain.* Highlands, i.e., land units higher than
257 80m in elevation, and hilly terrain, i.e., larger than 25 degrees in slope, were considered not
258 suitable for urban developments. The 80m was selected as the 95 percentiles of the
259 elevation values of existing urban lands. The 25 degrees was set according to local

260 government regulations.

261 3. *Waterbody and croplands are preserved.* No changes were allowed to existing water body
262 due to their essential ecological benefits. Croplands are also preserved to secure urban food
263 supply.

264

265 The objectives and constraints can be denoted as follows:

266 Minimize $LST_d = \sum_{i=1}^N f_d(I_{1,i}, I_{2,i}, \dots, I_{k,i})$

267 Minimize $LST_n = \sum_{i=1}^N f_n(I_{1,i}, I_{2,i}, \dots, I_{k,i})$

268 Minimize $numChanges = \sum_{i=1}^N [L'_i \neq L_i]$

269 Maximize $landUseCompatibility = \sum_{lm} (P_{lm} \cdot P'_{lm})$

270

271 Subject to,

272
$$\sum_{i=1}^N [L'_i \in \mathbf{U}] \geq \sum_{i=1}^N [L_i \in \mathbf{U}] \times (1 + r_g)$$

273
$$\frac{1}{N} \sum_{i=1}^N ISA'_i \geq \frac{1}{N} \sum_{i=1}^N ISA_i$$

274
$$\forall L_i \in \mathbf{U} : e_i < 80m; s_i < 25^\circ$$

275

276 The warming impacts of optimized climate-conscious urban growth plans were evaluated using the
277 same temperature-land-use relationship for evaluating unplanned urban growth plans. The
278 differences between the warming impacts of the unplanned urban growth and climate-conscious
279 urban growth were extracted to demonstrate the effectiveness of the CUGP as an urban warming
280 mitigation measure. The efficiency of the optimized changes is also measured using an indicator
281 that measures the LST change per proposed land-use change ($\overline{\Delta LST}$),

282

283
$$\overline{\Delta LST} = \frac{\sum_i (LST'_i - LST_i)}{numChanges} \quad (Eq. 3)$$

284

285 where i indicates cell locations within the study area.

286

287 3. RESULTS

288 **3.1 The estimated LST-land-use relationships.** By considering the spatially varying effects, the
289 spatially explicit models for both LST_d and LST_n fit the observations significantly better than their
290 corresponding spatially fixed models and therefore provide more accurate predictions of LSTs
291 (Section S2.1 for detailed results). The spatially explicit models provide good model fittings for
292 both LST_d ($R^2 = 0.810$) and LST_n ($R^2 = 0.725$), while the spatially fixed model has a fair model
293 fitting for LST_d ($R^2 = 0.537$) and a poor model fitting for LST_n ($R^2 = 0.275$). Since the spatially

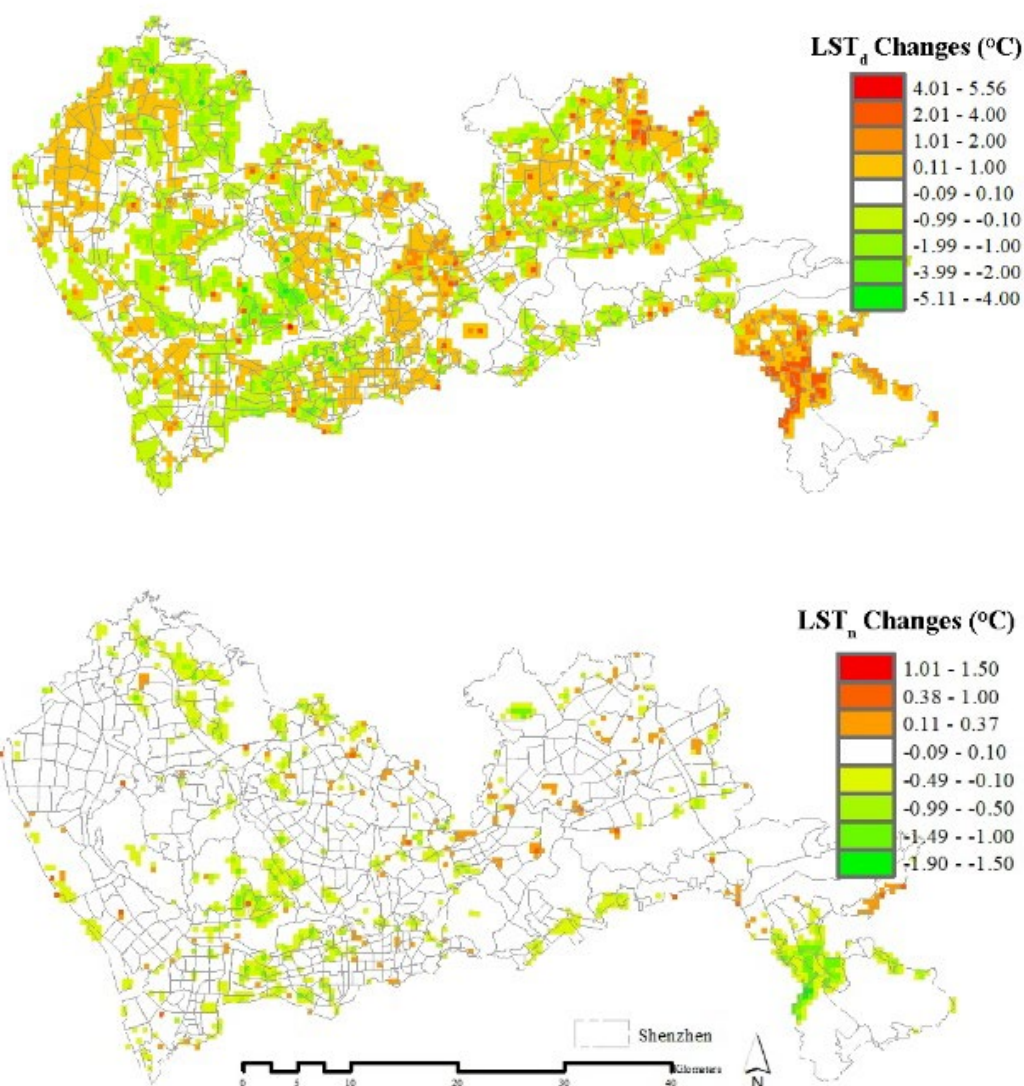
294 explicit models significantly outperform the spatially fixed models, they are selected as the objective
295 functions for assessing the warming impacts of urban land-use changes in the following SMOLA
296 model.

297

298 **3.2 Cost-Effectiveness of the CUGP.** Our evidence in Shenzhen, China shows that the CUGP can
299 be an effective urban climate mitigation measure. Both with 10% more urban lands, the unplanned
300 urban growth in the baseline scenario increased the average LST_d in Shenzhen by 0.21°C , while in
301 the experiment scenario, climate-conscious urban growth increased the average LST_d by 0.14°C ,
302 which is $0.07 \pm 0.01^\circ\text{C}$ ($33.8 \pm 4.6\%$) less warming impacts. Results from the t-test showed that the
303 0.07°C difference was statistically significant ($p < 0.005$).

304

305 The 0.07°C difference is not the cooling benefit on a single land unit; rather, it is the average cooling
306 benefit averaged over all land units in Shenzhen. The cooling efficiency of each optimized land-use
307 change is much more significant. The daytime $\overline{\Delta LST}$ (Eq. 3) is $-1.24^\circ\text{C}/\text{change}$, and the nighttime
308 $\overline{\Delta LST}$ is $-0.52^\circ\text{C}/\text{change}$. The CUGP is more effective during the daytime, since the LST_d is more
309 variable and sensitive to land-use changes. Despite the diurnal trade-offs between LST_d and LST_n ,
310 such decrease in LST_d was not achieved at the sacrifice of LST_n , in fact, LST_n also decreased an
311 average of 0.03°C after the optimization. Figure 2 maps daytime and nighttime LST changes caused
312 by the CUGP.



313

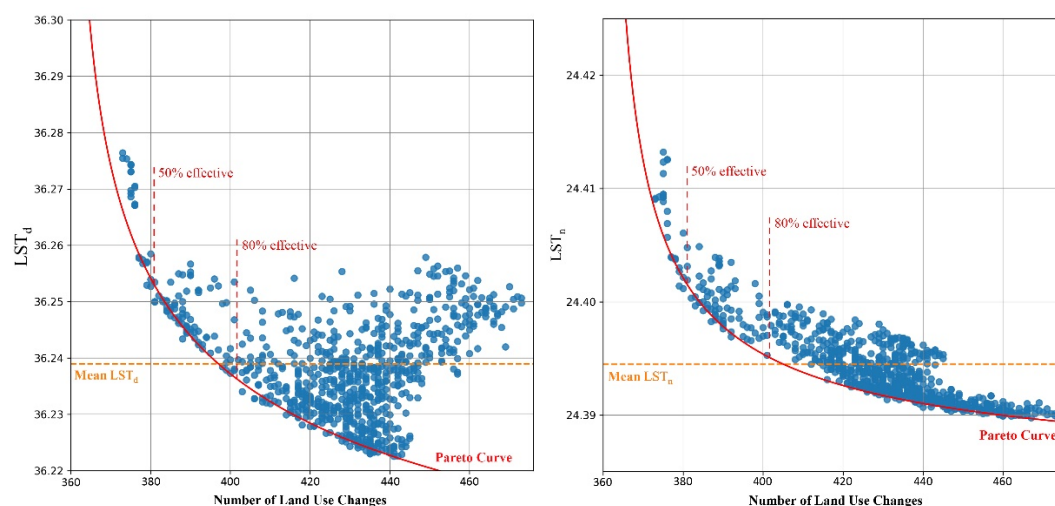
314

315 *Figure 2 Changes in daytime LST (LST_d) and nighttime LST (LST_n) introduced by the CUGP, compared with*
316 *warming impacts of unplanned urban growth.*

317

318 In addition, we examined the cost-effectiveness of the CUGP (Figure 3). The effectiveness of the
319 CUGP grows non-linearly as the number of changes increases. We took the lowest average LST_d
320 and LST_n among all optimized urban growth plans as the optimal mitigation performance that can
321 be achieved with the CUGP regardless of the number of land-use changes. To achieve 80% of the
322 optimal effectiveness in both LST_d and LST_n requires at least 56% of land-use changes. To achieve
323 50% of the optimal effectiveness in both LST_d and LST_n requires at least 25% of land-use changes.

324



325

326 *Figure 3 Cost-effectiveness of the CUGP for mitigating LST_d (left) and LST_n (right). Both two-dimensional Pareto*
327 *fronts can be fitted almost perfectly with a Pareto curve ($R^2 > 0.95$). Minimum changes required to achieve 50% and*
328 *80% of the optimal effectiveness for both LST_d and LST_n are also marked.*

329

330 4. Discussions

331 **4.1 Variances in the LST-land-use relationship.** The estimated LST-land-use relationships
332 substantially vary spatially, diurnally and compositionally. Our findings in the context of EHEs
333 agree with existing studies on regular hot days^{18,43} that substantial spatial variances exist in the LST-
334 land-use relationships, especially for such high-impact land-use types as high-density urban lands.
335 The responses of both daytime and nighttime LSTs can be profoundly affected by compositions of
336 the urban lands, such as the development densities^{19,44}, due to the so-called “canyon effect”¹⁵. The
337 reduced air ventilation determined by local energy balance and stability prevents the heat from
338 leaving the urban canopy layer trapping heat even after sunset.

339

340 However, this effect is not always true. For some areas in Shenzhen on the southeast coast, high-
341 density urban lands are found to contribute negatively to the nighttime LST. High-rise structures in
342 densely built-up areas could reduce the amount of insolation from getting into the urban canopy.
343 Also, the most important meteorological variable that alters the urban heat island effect is wind
344 speed¹⁵. The identified areas in Shenzhen are located on the seaside, where the local thermal
345 environment could benefit largely from the good air ventilation driven by sea and land breezes
346 allowing urban areas to cool down swiftly after sunset. Such ‘unexpected’ phenomena further
347 demonstrate the necessity of considering the varying effects, especially when dealing with spatial
348 data and environmental phenomena such as urban warming.

349

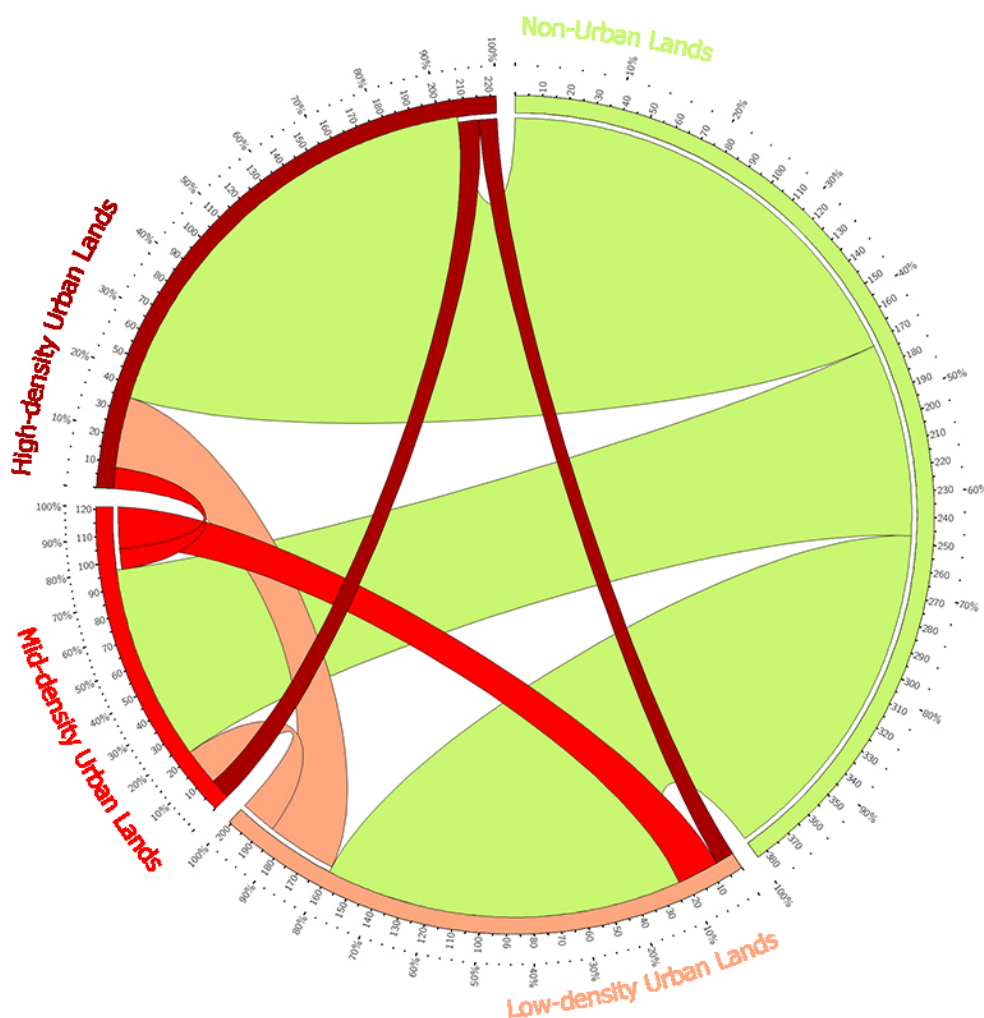
350 **4.2 Policy Implications of climate-conscious urban growth.** Our results agree with Stone et al.⁴
351 that cities with a greater urban sprawl would be more vulnerable to EHEs. However, beyond that,
352 our evidence suggests that not only the magnitude but also the spatial arrangement of urban growth
353 matters to the associated warming impacts. We further summarize the dominant ($P \geq 0.5$) change

354 for each spatial location from the *Pareto-optimal* solutions and analyzed their structural (Figure 4)
355 and spatial (Figure 5) patterns to provide suggestions for urban planners and researchers.

356

357 Structurally, climate-conscious urban growth in Shenzhen emphasizes compact urban development
358 for minimal warming impacts (Figure 4). The CUGP introduces substantially more high-density
359 (44.8%) and low-density (35.7%) urban lands than mid-density urban land (19.5%).

360



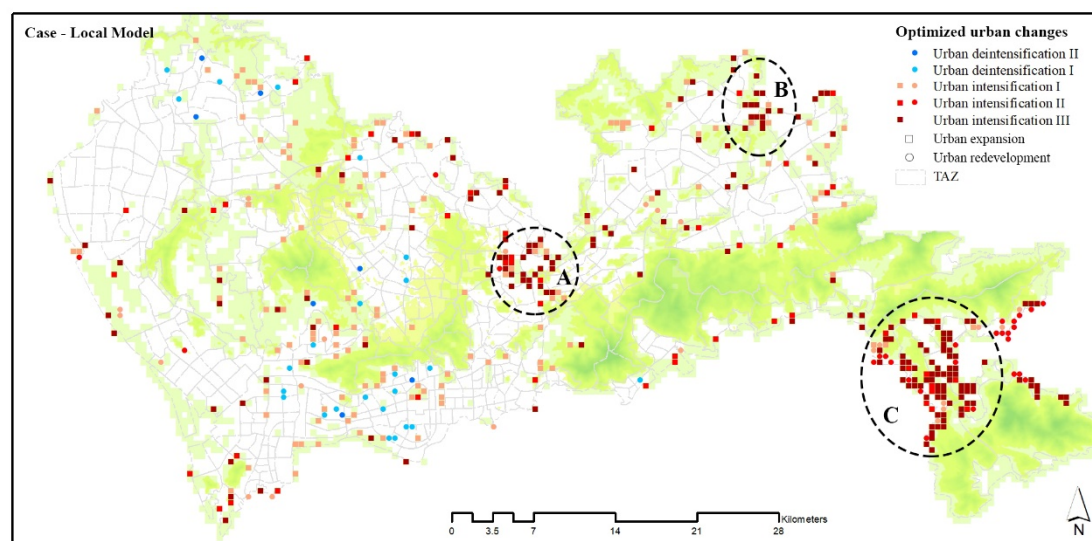
361

362 *Figure 4* The structure of dominant land-use changes ($P \geq 0.5$) optimized by the CUGP, visualized as incoming and
363 outgoing flows among the urban and non-urban land-use types using a circular plot⁴³. Numbers on the inner circle
364 indicate numbers of land parcels, while numbers on the outer circle are percentages of changed land parcels out of
365 all land parcels in each land-use category.

366 Climate-conscious urban growth in Shenzhen also suggests a spatially equalized distribution of
367 urban growth by locating more urban developments in the less-developed east half of Shenzhen
368 (Figure 5). The centers of the optimized urban growth move eastward by an average of 19.1km
369 compared to the random urban growth (Figure S5). By optimizing the spatial positioning of urban
370 lands, the CUGP also maximizes the mitigation effects of existing cooling sources in the city,

371 including green space and water bodies. The percentages of cooling sources surrounding high-
372 density and mid-density urban lands are increased by the CUGP (Table S5, SI). Clusters of new
373 urban lands (A, B, and C in Figure 5) are located adjacent to vast green spaces or water bodies. Such
374 a spatial pattern suggests that “cooling sources” should be established and preserved even in
375 compact cities. With sufficient “cooling sources”, the CUGP could efficiently mitigate urban
376 climate impacts of urban growth by locating compact urban development in places with sizeable
377 biological capacity, ideal weather conditions, and room for urban growth.

378



379

380 *Figure 5. The spatial distribution of dominant urban changes ($P \geq 0.5$) optimized by the CUGP. The changes are*
381 *classified as the urban expansion, i.e., urban development on newly acquired urban land, and urban redevelopment*
382 *on existing urban land. Both categories are reclassified into several levels of urban intensification and urban*
383 *deintensification to reflect the changes in urban densities (Table S4).*

384

385 **4.3 Model Sensitivity.** We further examined the sensitivity of the mitigation effect using different
386 combinations of model parameters. We repeated the analysis using three urban growth rates (10%,
387 20%, and 30%) and two elevation thresholds (80m and 120m). Results from the sensitivity analysis
388 (Table S3) show that the mitigation effects were statistically significant ($p < 0.005$) using all the 12
389 parameter combinations. Please refer to Section S2.2.2 for more details.

390

391 **4.4 Future Perspectives and Limitations**

392 Unlike the simple and universal rules in the game of Go, real-world environmental problems are far
393 more complex and include substantial spatio-temporal heterogeneities. Our results also show that
394 artificial intelligence algorithms are highly sensitive to model specifications and need to work in a
395 better-represented real-world settings.

396

397 For future directions, more evidence on the effectiveness of CUGP as an urban warming mitigation
398 measure may still be needed, especially from cities of the developing world where massive urban
399 growth is expected to occur, and local people are particularly vulnerable to extreme heat exposures.

400 Moreover, since our objective is to investigate the optimal effectiveness of the CUGP, the effects
401 of property rights, land markets, local land policies such as the Basic Ecological Control Line, and
402 community benefits are not considered. Integrating the afore-mentioned factors in the investigation
403 would provide more feasible land-use plans.

404

405

406 **Supporting Information**

- 407 • Supporting details about the experimental design, land-use map pre-processing, and the
408 NSGA-II based SMOLA model.
- 409 • Detailed results from the LST-land-use relationship estimation, land-use optimization, and
410 parameter sensitivity analysis.

411

412

413 **References**

- 414 (1) Howard, L. The Climate of London. *Int. Assoc. Urban Clim.* **1833**, 285.
- 415 (2) Sharifi, E.; Lehmann, S. Comparative Analysis of Surface Urban Heat Island Effect in Central
416 Sydney. *J. Sustain. Dev.* **2014**, *7* (3), 23–34.
- 417 (3) Peng, S.; Piao, S.; Ciais, P.; Friedlingstein, P.; Ottle, C.; Bréon, F. M.; Nan, H.; Zhou, L.; Myneni,
418 R. B. Surface Urban Heat Island across 419 Global Big Cities. *Environ. Sci. Technol.* **2012**, *46*
419 (2), 696–703.
- 420 (4) Stone, B.; Hess, J. J.; Frumkin, H. Urban Form and Extreme Heat Events: Are Sprawling Cities
421 More Vulnerable to Climate Change than Compact Cities? *Environ. Health Perspect.* **2010**, *118*
422 (10), 1425–1428.
- 423 (5) Chen, Z.; Xie, X.; Cai, J.; Chen, D.; Gao, B.; He, B.; Cheng, N.; Xu, B. Understanding
424 Meteorological Influences on PM_{2.5} Concentrations across China: A Temporal and Spatial
425 Perspective. *Atmos. Chem. Phys.* **2017**, *0086* (0086), 1–30.
- 426 (6) Rizwan, A. M.; Dennis, L. Y. C.; Liu, C. A Review on the Generation, Determination and
427 Mitigation of Urban Heat Island. *J. Environ. Sci.* **2008**, *20* (1), 120–128.
- 428 (7) Santamouris, M. Using Cool Pavements as a Mitigation Strategy to Fight Urban Heat Island - A
429 Review of the Actual Developments. *Renewable and Sustainable Energy Reviews.* 2013, pp 224–
430 240.
- 431 (8) Santamouris, M. Cooling the Cities - A Review of Reflective and Green Roof Mitigation
432 Technologies to Fight Heat Island and Improve Comfort in Urban Environments. *Sol. Energy*
433 **2014**, *103*, 682–703.
- 434 (9) Kolokotsa, D.; Santamouris, M.; Zerefos, S. C. Green and Cool Roofs' Urban Heat Island
435 Mitigation Potential in European Climates for Office Buildings under Free Floating Conditions.
436 *Sol. Energy* **2013**, *95*, 118–130.
- 437 (10) Akbari, H.; Kolokotsa, D. Three Decades of Urban Heat Islands and Mitigation Technologies
438 Research. *Energy Build.* **2016**, *133*, 834–852.
- 439 (11) Zhang, W.; Huang, B. Land Use Optimization for a Rapidly Urbanizing City with Regard to

- 440 Local Climate Change: Shenzhen as a Case Study. *J. Urban Plan. Dev.* **2014**, *141* (1), 5014007.
- 441 (12) Zhang, Y.; Murray, A. T.; Turner, B. L. Optimizing Green Space Locations to Reduce Daytime
442 and Nighttime Urban Heat Island Effects in Phoenix, Arizona. *Landsc. Urban Plan.* **2017**, *165*,
443 162–171.
- 444 (13) Heaviside, C.; Vardoulakis, S.; Cai, X. X.-M. Attribution of Mortality to the Urban Heat Island
445 during Heatwaves in the West Midlands, UK. *Environ. Heal.* **2016**, *15* (S1), S27.
- 446 (14) Urban Growth. In *The New Palgrave Dictionary of Economics*; Durlauf, S. N., Blume, L. E.,
447 Eds.; Nature Publishing Group: Basingstoke, 2008; pp 544–546.
- 448 (15) Oke, T. R. The Energetic Basis of the Urban Heat Island. *Q. J. R. Meteorol. Soc.* **1982**, *108* (455),
449 1–24.
- 450 (16) Buyantuyev, A.; Wu, J. Urban Heat Islands and Landscape Heterogeneity: Linking
451 Spatiotemporal Variations in Surface Temperatures to Land-Cover and Socioeconomic Patterns.
452 *Landsc. Ecol.* **2010**, *25* (1), 17–33.
- 453 (17) Zhou, W.; Huang, G.; Cadenasso, M. L. Does Spatial Configuration Matter? Understanding the
454 Effects of Land Cover Pattern on Land Surface Temperature in Urban Landscapes. *Landsc.*
455 *Urban Plan.* **2011**, *102* (1), 54–63.
- 456 (18) Zhou, X.; Wang, Y. C. Dynamics of Land Surface Temperature in Response to Land-Use/Cover
457 Change. *Geogr. Res.* **2011**, *49* (1), 23–36.
- 458 (19) Imhoff, M. L.; Zhang, P.; Wolfe, R. E.; Bounoua, L. Remote Sensing of the Urban Heat Island
459 Effect across Biomes in the Continental USA. *Remote Sens. Environ.* **2010**, *114* (3), 504–513.
- 460 (20) Wang, J.; Huang, B.; Fu, D.; Atkinson, P. M.; Zhang, X. Response of Urban Heat Island to Future
461 Urban Expansion over the Beijing-Tianjin-Hebei Metropolitan Area. *Appl. Geogr.* **2016**, *70*, 26–
462 36.
- 463 (21) Tewari, M.; Salamanca, F.; Martilli, A.; Treinish, L.; Mahalov, A. Impacts of Projected Urban
464 Expansion and Global Warming on Cooling Energy Demand over a Semiarid Region. *Atmos.*
465 *Sci. Lett.* **2017**, *18* (11), 419–426.
- 466 (22) Peng, J.; Xie, P.; Liu, Y.; Ma, J. Urban Thermal Environment Dynamics and Associated
467 Landscape Pattern Factors: A Case Study in the Beijing Metropolitan Region. *Remote Sens.*
468 *Environ.* **2016**, *173*, 145–155.
- 469 (23) Chapman, S.; Watson, J. E. M.; Salazar, A.; Thatcher, M.; McAlpine, C. A. The Impact of
470 Urbanization and Climate Change on Urban Temperatures: A Systematic Review. *Landsc. Ecol.*
471 **2017**, *32* (10), 1921–1935.
- 472 (24) Connors, J. P.; Galletti, C. S.; Chow, W. T. L. L. Landscape Configuration and Urban Heat Island
473 Effects: Assessing the Relationship between Landscape Characteristics and Land Surface
474 Temperature in Phoenix, Arizona. *Landsc. Ecol.* **2013**, *28* (2), 271–283.
- 475 (25) Zheng, B.; Myint, S. W.; Fan, C. Spatial Configuration of Anthropogenic Land Cover Impacts
476 on Urban Warming. *Landsc. Urban Plan.* **2014**, *130* (1), 104–111.
- 477 (26) Doan, V. Q.; Kusaka, H. Projections of Urban Climate in the 2050s in a Fast-Growing City in
478 Southeast Asia: The Greater Ho Chi Minh City Metropolitan Area, Vietnam. *Int. J. Climatol.*
479 **2018**, *38* (11), 4155–4171.

- 480 (27) Kusaka, H.; Suzuki-Parker, A.; Aoyagi, T.; Adachi, S. A.; Yamagata, Y. Assessment of RCM
481 and Urban Scenarios Uncertainties in the Climate Projections for August in the 2050s in Tokyo.
482 *Clim. Change* **2016**, *137* (3–4), 427–438.
- 483 (28) Schlager, K. J. A Land Use Plan Design Model. *J. Am. Plan. Assoc.* **1965**, *31* (2), 103–111.
- 484 (29) Cooper, L. Location-Allocation Problems. *Oper. Res.* **2008**, *11* (3), 303–473.
- 485 (30) Wright, J. J.; Reville, C.; Cohon, J.; Cohon Jared. A Multiobjective Integer Programming Model
486 for the Land Acquisition Problem. *Reg. Sci. Urban Econ.* **1983**, *13*, 31–53.
- 487 (31) Stewart, T. J.; Janssen, R.; van Herwijnen, M. A Genetic Algorithm Approach to Multiobjective
488 Land Use Planning. *Comput. Oper. Res.* **2004**, *31* (14), 2293–2313.
- 489 (32) Ligmann-Zielinska, A.; Church, R.; Jankowski, P. Spatial Optimization as a Generative
490 Technique for Sustainable Multiobjective Land-Use Allocation. *Int. J. Geogr. Inf. Sci.* **2008**, *22*
491 (6), 601–622.
- 492 (33) Janssen, R.; van Herwijnen, M.; Stewart, T. J.; Aerts, J. C. J. H. Multiobjective Decision Support
493 for Land-Use Planning. *Environ. Plan. B Plan. Des.* **2008**, *35* (4), 740–756.
- 494 (34) Cao, K.; Batty, M.; Huang, B.; Liu, Y.; Yu, L.; Chen, J. Spatial Multi-Objective Land Use
495 Optimization: Extensions to the Non-Dominated Sorting Genetic Algorithm-II. *Int. J. Geogr. Inf.*
496 *Sci.* **2011**, *25* (12), 1949–1969.
- 497 (35) Aerts, J. C. J. H.; Eisinger, E.; Heuvelink, G. B. M.; Stewart, T. J. Using Linear Integer
498 Programming for Multi-Site Land-Use Allocation. *Geogr. Anal.* **2003**, *35* (2), 148–169.
- 499 (36) Balling, R. J.; Taber, J. T.; Brown, M. R.; Day, K. Multiobjective Urban Planning Using Genetic
500 Algorithm. *J. Urban Plan. Dev.* **2002**, *125* (2), 86–99.
- 501 (37) Xiao, N.; Bennett, D. A.; Armstrong, M. P. Using Evolutionary Algorithms to Generate
502 Alternatives for Multiobjective Site-Search Problems. *Environ. Plan. A* **2002**, *34* (4), 639–656.
- 503 (38) Chandramoull, M.; Huang, B.; Xue, L. Spatial Change Optimization: Integrating GA with
504 Visualization for 3D Scenario Generation. *Photogramm. Eng. Remote Sensing* **2009**, *75* (8),
505 1015–1022.
- 506 (39) Huang, B.; Zhang, W. Sustainable Land-Use Planning for a Downtown Lake Area in Central
507 China: Multiobjective Optimization Approach Aided by Urban Growth Modeling. *J. Urban*
508 *Plan. Dev.* **2014**, *140* (2).
- 509 (40) Luo, M.; Lau, N. C. Heat Waves in Southern China: Synoptic Behavior, Long-Term Change,
510 and Urbanization Effects. *J. Clim.* **2017**, *30* (2), 703–720.
- 511 (41) Wan, Z. New Refinements and Validation of the Collection-6 MODIS Land-Surface
512 Temperature/Emissivity Product. *Remote Sens. Environ.* **2014**, *140*, 36–45.
- 513 (42) Nakaya, T.; Fotheringham, S.; Charlton, M.; Brunson, C. Semiparametric Geographically
514 Weighted Generalised Linear Modelling in GWR4.0. In *Proceedings of Geocomputation 2009*;
515 2009; pp 1–5.
- 516 (43) Su, Y.-F.; Foody, G. M.; Cheng, K.-S. Spatial Non-Stationarity in the Relationships between
517 Land Cover and Surface Temperature in an Urban Heat Island and Its Impacts on Thermally
518 Sensitive Populations. *Landsc. Urban Plan.* **2012**, *107* (2), 172–180.
- 519 (44) Zhou, D.; Zhao, S.; Liu, S.; Zhang, L.; Zhu, C. Surface Urban Heat Island in China's 32 Major

- 520 Cities: Spatial Patterns and Drivers. *Remote Sens. Environ.* **2014**, *152*, 51–61.
- 521 (45) Abel, G. J.; Sander, N. Quantifying Global International Migration Flows. *Science (80-.)*. **2014**,
- 522 *343* (6178), 1520–1522.
- 523